

Complete many-body localization in the t - J model caused by random magnetic field

Gal Lemut,¹ Marcin Mierzejewski,² and Janez Bonča^{3,1}

¹*J. Stefan Institute, 1000 Ljubljana, Slovenia*

²*Department of Theoretical Physics, Faculty of Fundamental Problems of Technology,
Wrocław University of Science and Technology, 50-370 Wrocław, Poland*

³*Faculty of Mathematics and Physics, University of Ljubljana, 1000 Ljubljana, Slovenia*

The many body localization (MBL) of spin-1/2 fermions poses a challenging problem. It is known that the disorder in the charge sector may be insufficient to cause full MBL. Here, we study dynamics of a single hole in one dimensional t - J model subject to a random magnetic field. We show that strong disorder that couples only to the spin sector localizes both spin and charge degrees of freedom. Charge localization is confirmed also for a finite concentration of holes. While we cannot precisely pinpoint the threshold disorder, we conjecture that there are two distinct transitions. Weaker disorder first causes localization in the spin sector. Carriers become localized for somewhat stronger disorder, when the spin localization length is of the order of a single lattice spacing.

PACS numbers: 71.23.-k, 71.27.+a, 71.30.+h, 71.10.Fd

Introduction.— The many-body localization (MBL) has been demonstrated by various numerical [1–11] and analytical studies [12, 13] carried out mostly for one-dimensional (1D) systems of spinless particles or equivalent spin-models. Among unusual properties of MBL we only emphasize the logarithmic growth of the entanglement entropy [14–20], and the subdiffusive transport in the regime of strong disorder but still below the MBL transition [21–24].

While MBL is well understood for the simplest Hamiltonians, it is essential to recognize the class of more realistic quantum systems which may host this extraordinary phase. A challenging question concerns the dynamics of disordered two-dimensional interacting systems [25–27] and 1D Hamiltonians which account for spin [28–33] or lattice degrees of freedom [34, 35]. Numerical studies of the 1D Hubbard model [29] suggest that the disorder strength needed for localization is very large. Other results [28] obtained for the same model indicate that strong disorder in the charge sector localizes only charge carriers, while spin excitations remain delocalized. Similar studies carried out for the t - J model [32] suggest that localization of these carriers should be accompanied by localization of the spin degrees of freedom, otherwise the charge dynamics is subdiffusive up to the longest times accessible to the numerical calculations. Such expectation may be supported also by the studies in Refs. [30, 31].

A general problem concerns the dynamics of a multicomponent system in the presence of disorder which couples exclusively to one of its subsystems. There is a quite convincing evidence that all subsystems [32, 34] or at least some of them [28] may be delocalized. However, can such system show complete MBL where all degrees of freedom are localized? In this work we show that it is indeed possible. We consider a Hamiltonian, which is very similar to that in Ref. [36], namely, we study one-dimensional t - J model. However, the disorder is introduced not in the charge sector but in the spin sector through a random magnetic field [37] breaking the $SU(2)$ symmetry [38–40]. We show that such disorder may localize both charge and spin degrees of freedom. We specu-

late also that there may be two localization transitions, one for spin and the other for charge degrees of freedom.

Model and method. In the first part we investigate 1D t - J model with a single hole in a random external magnetic field $h_i \in [-W, W]$

$$H = -t_0 \sum_{i,\sigma} \tilde{c}_{i,\sigma}^\dagger \tilde{c}_{i+1,\sigma} + c.c. + J \sum_i \mathbf{S}_i \mathbf{S}_{i+1} + \sum_i h_i S_i^z, \quad (1)$$

where $\tilde{c}_{i,\sigma} = (1 - n_{i,-\sigma})c_{i,\sigma}$ is a projected fermion operator. We perform calculations for various length sizes L and open boundary conditions. We perform time-evolution using Lanczos based technique. For most cases we use complete Hilbert spaces with a fixed total $S^z = 0$. When computing the time evolution of the initially localized hole we use the limited functional Hilbert space (LFS) [41–44]. This method enabled calculations on larger chains up to a maximal size $L_{\max} = 29$, described in more details in Ref. [45].

We start the time evolution from a Néel background, with the hole located in the middle of the chain. In addition we compute static expectation values of various physical quantities for eigenstates in the middle of the energy band using ARPAZ Lanczos techniques. We typically take 500 realizations of the disorder. We measure time in units of $[1/t_0]$ and set $t_0 = 1$. If not specified otherwise, we set also $J = 1$.

In order to investigate the dynamics of the charge carrier we calculate the hole density

$$\rho_i = \langle \psi | 1 - n_{i\uparrow} - n_{i\downarrow} | \psi \rangle_{\text{ave}}, \quad (2)$$

where $\langle \rangle_{\text{ave}}$ signifies that expectation values have been averaged over different random realizations of h_i . We also define the mean square deviation of the hole distribution [46]

$$\sigma^2 = \sum_i i^2 \rho_i - \left[\sum_i i \rho_i \right]^2. \quad (3)$$

Figure 1(a) shows ρ_i computed at large time of evolution, e.g. $t = 200$. Note that for $t = 0$, the initial density is $\rho_i =$

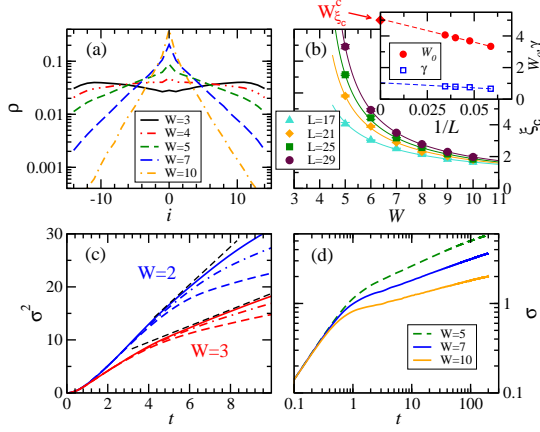


Figure 1. a) The hole density ρ_i at time $t = 200$ for different values of W as indicated in the insert. The size of the system was $L = 29$; b) extracted charge localization lengths ξ_c for different system sizes vs. W . Thin lines represent fits of the form $\xi_c = A/(W - W_0)^\gamma$. Insert: fit parameters extrapolated towards $1/L = 0$; c) $\sigma^2(t)$ for short times below the localization transition, $W = 2$ and 3 showing diffusive behavior. Thin black dashed straight lines are guides to the eye. Dashed, dot-dashed and full lines represent system sizes $L = 21, 25$, and 29 , respectively; d) $\sigma(t)$ on $\log(t)$ scale for $W = 5, 7$, and 10 for maximal system size $L = 29$ using LFS.

δ_{i0} . At small $W = 2$ and 3 results are consistent with the delocalized state of the hole. In contrast, for $W \geq 5$, ρ_i is compatible with the localized state, $\rho_i \sim \exp(-|i|/\xi_c)$ for $i \neq 0$. Extracted charge localization lengths ξ_c are presented in Fig. 1(b) for different system sizes L as functions of W . Functional dependence of $\xi_c(W)$ can be well fitted using a divergent form as described $\xi_c = A/(W - W_c)^\gamma$. After $L \rightarrow \infty$ scaling we obtain a threshold value $W_c^c \simeq 5$ separating delocalized regime (for $W < W_c^c$) from localized one. Since the charge dynamics doesn't saturate for $t \leq 200$, see Fig. 1d, while ξ_c increases with time, we conclude that for $t \rightarrow \infty$ one gets $W_c^c \gtrsim 5$.

While the exponent $\gamma \simeq 1$ is consistent with other results for spinless fermions (or equivalent spin model) [3, 18, 47, 48], it violates the so-called Harris-Chayes bound (HCB) $\gamma > 2$ [49, 50]. However, RG calculations predict a much larger $\gamma \approx 3.5$ [51, 52] consistent with the HCB. Violation of the HCB may originate from absence of a unique length-scale [48].

We next follow the hole dynamics via $\sigma^2(t)$. In Fig. 1(c) we show short-time results for small values of $W = 2$ and 3 . We observe linear increase of $\sigma^2(t)$, consistent with the diffusive spread of the initially localized hole. At large values of $W = 5, 7$, and 10 as shown in Fig. 1(d), we observe a subdiffusive propagation of the hole, $\sigma^2(t) \propto t^\alpha$ where the exponent $\alpha < 1$ decreases with increasing W . Eventually, for very large disorder, α becomes so small that the latter dependence is indistinguishable from the logarithmic increase of $\sigma(t)$ that is compatible with the proximity to the MBL state [53].

Next, we check whether some particular realizations of

disorder cause localization of the hole. We have thus fitted $\sigma^2(t) \propto t^\alpha$ independently for each realization of the disorder and obtained the distribution of the exponents $f(\alpha)$. We took special care to perform fits in the time domain free of finite-size effects. In Fig. 2(a) we show the cumulative distribution function,

$$F(\alpha) = \int_0^\alpha d\alpha' f(\alpha'), \quad (4)$$

We find $F(\alpha \rightarrow 0) = 0$ for $W < 5$ while $F(\alpha \rightarrow 0) = F_0 > 0$ for $W = 7$ and 10 , which indicates localization.

We have also computed σ for the case when $|\psi\rangle$ in Eq. (2) are eigenstates of the Hamiltonian taken from the middle of the energy spectrum. In Fig. 2(b) we show $1/\sigma$ scaling of $1/\sigma$. We can clearly see the transition from delocalized states where $1/\sigma(L \rightarrow \infty) \rightarrow 0$ for $W \lesssim 4.0$ towards localized ones with $1/\sigma(L \rightarrow \infty) \rightarrow 1/\sigma_0 > 0$ for $W \gtrsim 5.0$. In the inset we show scaling of extrapolated values σ_0 with W together with a fit $\sigma_0 \propto 1/(W - W_c^c)^\gamma$, which allows one to locate the divergence of σ_0 at $W_c^c \simeq 5$. Another signature of the MBL transition is observed in variance (with respect to different realizations of disorder) of $\Delta\sigma/L$, presented in Fig. 2(c) that shows a peak around $W \simeq 5$. Exactly at the transition we observe a linear scaling of $\Delta\sigma$ with L and, consequently, $\Delta\sigma(W)/L$ becomes narrower as the system size increases.

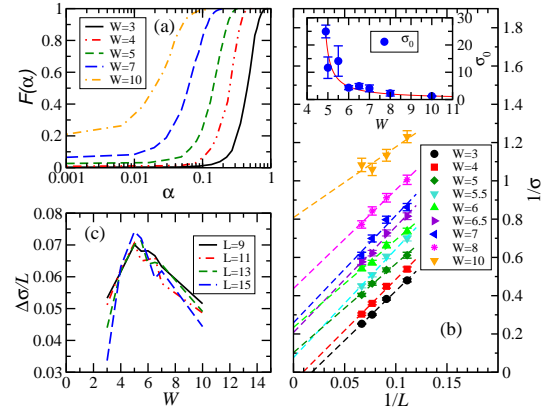


Figure 2. a) $F(\alpha)$ for different values of W . The largest available LFS Hilbert space with $L = 29$ was used in this case; b) $1/\sigma$ scaling with the system size L . Insert: extrapolated values σ_0 (circles) with a fit (full line) on the functional form $\sigma_0 \propto 1/(W - W_c^c)^\gamma$ with $W_c^c \simeq 5$ and $\gamma \simeq 0.95$; c) variance of σ for different system sizes L . Calculations in (b) and (c) were performed from eigenstates from the middle of the energy spectrum using complete Hilbert spaces.

The hole becomes localized at $W^c \simeq 5$ even though it is not directly subject to a random potential. We expect the localization of spin dynamics with increasing W in the thermodynamic limit at the same value of $W^s \sim 3.7 \pm 0.5$ as in the undoped case [3, 54, 55], since a single hole can not influence the transition of an infinite chain. We test this idea by computing the entanglement entropy $S = -\sum_\lambda w_\lambda \log w_\lambda$

where w_λ are eigenvalues of the reduced density matrix of a subsystem. Since we work with odd system sizes, we have defined the reduced density matrix over a subsystem of length $L_a = (L + 1)/2$. While the subsystem contains spin as well as charge degrees of freedom, it is important to stress that there are only L_a different states in the subsystem for the hole in contrast there is exponentially more spin degrees of freedom. In the thermodynamic limit the entanglement entropy thus measures predominantly the entropy of the spin sector.

The time evolution of the entanglement entropy shows a slow growth for $W \gtrsim 5$, *i.e.* $S(t)/L \sim \log(t)$, as displayed in Fig. 3(a), which is consistent with the MBL state [14, 17]. In contrast, for small $W = 1$ and 2, S/L_a on a time scale $\tau \sim 10 - 50$ approach a constant slightly below $\log(2)$, which represents infinite- T limit of an undoped spin-one-half chain in a thermal state. Transition between delocalized to localized regime can be well captured as well by following the size-dependence of the entanglement entropy S/L_a , [3]. In Fig. 3(b) we show S/L_a vs. W of the half-chain system obtained from eigenstates from the middle of the energy spectrum for different system sizes. We observe a crossover around $W^s \simeq 4$ as the system crosses over from the volume-law, characteristic for ergodic and delocalized systems, towards the area-law, that signals localization as the subsystem size exceeds the localization length. In addition we show in Fig. 3(c) the variance of the entanglement entropy $\Delta S/L_a$ that shows broad peak centered around $W^s \simeq 4$.

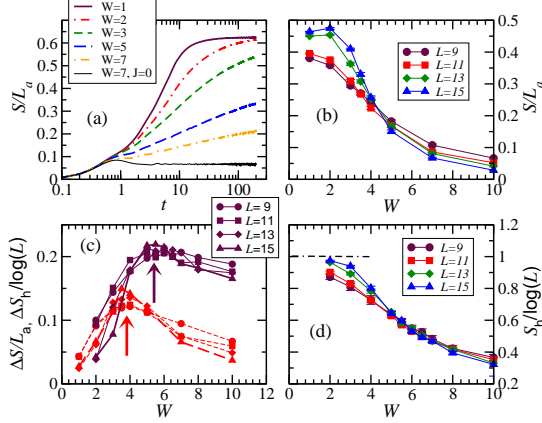


Figure 3. a) S/L_a for various values of W . Results were computed using a complete basis on $L = 13$ sites chain. Time evolution started from a Néel state with hole located in the middle of the chain. Thin black line represents Anderson's localized state for $W = 7$ and $J = 0$; b) S/L_a computed from eigenstates from the middle of the energy band. The same holds for (c) and (d). Results are shown for various chain lengths, $L = 9, 11, 13$, and 15 ; c) the variance of S and S_h (symbols connected with dashed and full lines respectively) vs. W ; d) hole entropy S_h for different system sizes L .

To gain additional insight into the localized phase we trace out the spin degrees of freedom and obtain a reduced density matrix for the charge carrier. Consequently, the resulting von Neumann entropy, S_h , quantifies entanglement between the

spin and the charge degrees of freedom. Deep in the MBL phase the charge and spin excitations are weakly entangled (see Fig. 3(d)). Note also that the variance ΔS_h peaks at larger value of W than ΔS , see Fig. 3(c).

Our results support MBL at large values of $W \gtrsim 5$ in the charge as well as in the spin sector. While MBL in the spin sector is mostly expected based on many previous works [3, 14, 54, 55], the same is not true for the charge sector. An intuitive picture for the localization of the hole is obtained in the extreme anisotropic limit of the exchange interaction, *i.e.* in the limit when $J = J_z$ and even at $J = 0$. Then, the system evolves within a space spanned by the states, $|\psi_i\rangle = |s_1, s_2, \dots, s_{i-1}, 0_i, s_{i+1}, s_L\rangle$ with a frozen sequence (but not position) of $L - 1$ spins s_1, \dots, s_L . As a result, the dynamics maps onto a problem of a single particle in a random on-site potential ϵ_i where

$$\epsilon_i = \sum_{j \neq i} h_j s_j + J_z \sum_{j \neq i-1, i} s_j s_{j+1} \quad (5)$$

that is Anderson's localized at $W > 0$. As an example we present data for $S/L_a(t)$ for $J = 0$ in Fig. 3(a) displaying rapid saturation, characteristic for Anderson's localization. The picture of frozen Ising-like spins is oversimplified in the presence of many-body interactions. It doesn't account for slow (logarithmic in time) but non-negligible spin dynamics visible in Fig. 3(a) for $J \neq 0$. Nevertheless, this results brings us to the hypothesis that the localization of the hole must be caused by the localization of spin degrees of freedom. We discuss this problem in more details at the end of the manuscript as well as in the Supplemental Material [45].

Finite doping. The essential question is whether the randomness in the spin sector may induce the full MBL also for nonzero concentration of holes. It is very demanding to carry out reliable finite-size scaling for arbitrary concentration of carriers. A nontrivial but still numerically feasible case concerns the system with equal numbers ($L/3$) of holes, spin-up and spin-down electrons. Following Ref. [56] we investigate the charge imbalance P . We study time evolution of initial states such that every third lattice site (belonging to sublattice A) is occupied by holes whereas electrons are randomly distributed on the other sites which form the sublattice B . Then, P reads

$$P = \frac{3}{L} \left(\sum_{i \in A} \rho_i - \frac{1}{2} \sum_{i \in B} \rho_i \right). \quad (6)$$

The factor $1/2$ is the ratio of the number of sites in both sublattices. Initially all ($L/3$) holes occupy the sublattice A , hence $P(t = 0) = 1$. Figure 4(b) shows $P(t)$ where time propagation has been carried out using full Hilbert space. Charge localization means that the system retains information on the initial distribution of holes for arbitrarily long times, *i.e.*, $P(t \rightarrow \infty) > 0$. This is clearly observed in Fig. 4(a) where at $W \gtrsim 10$ even after finite size analysis, Ref. [45], $P(t)$ displays slow logarithmic decay, characteristic for MBL, *e.g.* see Ref. [53]. In contrast, in the delocalized phase

($W \lesssim 5$) $P(t \rightarrow \infty) \rightarrow 0$ while it starts to substantially deviate from 0 for $W \gtrsim 7$, Fig. 4(b). In the latter figure we show also results for smaller (more realistic) exchange interaction $J = 0.4$, when the charge localization is even more evident.

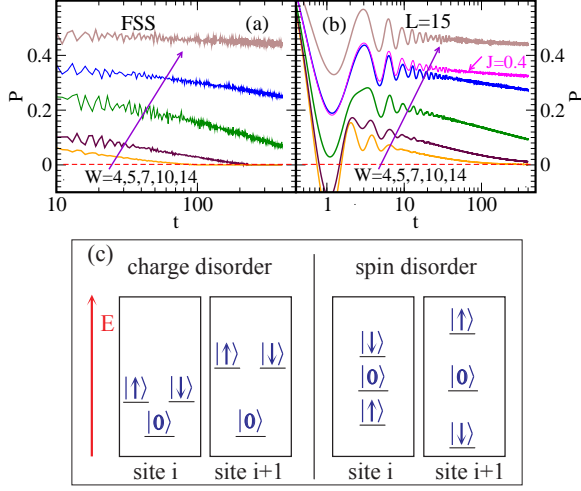


Figure 4. Time evolution of the charge imbalance $P(t)$ of the t - J model with L sites, $L/3$ holes and equal number of spin-up and spin-down Fermions. Results after finite size analysis are shown in a); b) results at fixed $L = 15$ and different values of W compared with data for $J = 0.4$ and $W = 10$; c) schematics portraying diagonal energies of the basis states on neighboring sites for the case of charge and spin disorder.

It is interesting that charge disorder is insufficient to induce full MBL[36], whereas random magnetic field can localize all degrees of freedom. Most probably, this difference originates from a specific structure of the Hilbert space which excludes double occupancy. At each site, the space is spanned by only three states $|\alpha_i\rangle$ with $\alpha = 0, \uparrow, \downarrow$. The disorder in the charge- and spin-sectors enter the Hamiltonian, respectively through terms $H'_{c,s} = \sum_i h_i (|\uparrow_i\rangle\langle\uparrow_i| \pm |\downarrow_i\rangle\langle\downarrow_i|)$, with random h_i . The basis states are eigenstates of $H'_{c,s}$, i.e., $H'_{c,s}|\alpha_i\rangle = E_{c,s}(\alpha)|\alpha_i\rangle$. However, for the charge disorder one finds degenerate eigenvalues $E_c(\uparrow) = E_c(\downarrow)$, whereas for spin disorder the spectrum $E_s(\alpha)$ is nondegenerate (see Fig. 4(c)). In the case of spin disorder, the change of energy due to arbitrary rearrangement of spins or charges, $|\alpha_i\alpha'_j\rangle\langle\alpha'_i\alpha_j|$ with $\alpha \neq \alpha'$, is of the order of W . Therefore, all degrees of freedom become localized for sufficiently strong disorder. However due to the degenerate spectrum obtained for charge disorder, the change of energy due to spin-flip $|\uparrow_i\downarrow_j\rangle\langle\downarrow_i\uparrow_j| + H.c.$ is independent of W and magnetic excitations may remain delocalized.

In summary we have shown that a system with coupled charge and spin degrees of freedom may undergo a complete MBL transition due to disorder which couples only to the spin sector. Here, the complete MBL is understood as a phase where both charge and spin excitations are localized. Support for this conclusion comes from numerical studies of the t - J

model in the low-doping regime and with random magnetic field. We have carried out complementary studies of several quantities which consistently show for $J = 1$ that the spin and charge degrees of freedom become localized when the magnitude of random field exceeds $W^s \simeq 4$ and $W^c \simeq 5$, respectively. While the main purpose of this work is just to show existence of the complete MBL, we conclude that our results may be consistent with two separate transitions (or crossovers) at W^s and $W^c > W^s$. The charge degrees are not localized until the spin localization length is of the order of a single lattice spacing. However, due to the proximity of both transitions, this conjecture should be verified by additional numerical studies. While thorough numerical studies have been carried out for vanishing concentration of holes, we have shown that for sufficiently strong disorder full MBL arises also for nonzero concentration of carriers.

J.B. acknowledges the financial support from the Slovenian Research Agency (research core funding No. P1-0044) and M.M. acknowledges support by the project 2016/23/B/ST3/00647 of the National Science Centre, Poland. This work was performed, in part, at the Center for Integrated Nanotechnologies, a U.S. Department of Energy, Office of Basic Energy Sciences user facility.

Supplemental Material

CALCULATION OF SPIN LOCALIZATION LENGTH ξ_s

In this section we show that for large enough W spin localization length ξ_s is smaller than the charge localization length ξ_c . To obtain an estimate of ξ_s we follow ideas by J. Hauschild *et al* [33] where they computed melting of a domain-wall in a spin-1/2 XXZ chain. In a similar fashion we prepare our system in a state where the left part of the chain ($j < 0$) with $(L_a - 1)$ -sites has spins oriented up, the right-side ($j > 0$) down, while the hole is placed in the middle at $j = 0$. We time evolve the system up to $t \sim 200$ and display results for $L = 13$ using full Hilbert space in Fig. S5. We observe smearing of the domain wall with an exponential decay of the spin redistribution penetrating the respective domains. By fitting of $\langle S_j^z \rangle$ with the exponential form, as shown in Fig. S5(b), we obtain $\xi_s = 1.1, 0.96$ and 0.71 for $W = 5, 7$ and 10 respectively, see Fig. S5(b). Comparing these results with ξ_c , presented in Fig. 1(b) of the main text, we indeed obtain $\xi_c > \xi_s$.

FINITE-SIZE SCALING OF 1/3 HOLE-DOPED t - J MODEL

Finite size scaling was performed on three different system sizes $L = 9, 12$, and 15 with identical hole doping $n_{\text{hole}} = 1/3$. In all cases full Hilbert spaces and periodic boundary conditions were used. In the case of finite doping, we have

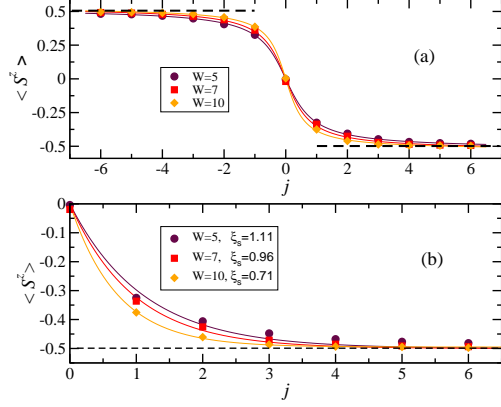


Figure S5. a) $\langle S_j^z \rangle(t = 200)$ for different values of $W > W^s$. Full lines represent guides to the eye while dashed horizontal lines represent values of $\langle S_j^z \rangle(t = 0)$; b) exponential fits with a single parameter ξ_s : $\langle S_j^z \rangle = -0.5(1 - \exp(-j/\xi_s))$ for $j \geq 0$. Results were obtained on a $L = 13$ system with complete Hilbert space.

studied a slightly modified version of t - J model:

$$H = -t_0 \sum_{i,\sigma} \tilde{c}_{i,\sigma}^\dagger \tilde{c}_{i+1,\sigma} + c.c. + J \sum_i (\mathbf{S}_i \mathbf{S}_{i+1} - n_i n_{i+1}/4) + \sum_i h_i S_i^z. \quad (\text{S7})$$

In the case of a single hole the term containing products of particle number operators $n_i n_{i+1}$ represent only a constant shift of the energy.

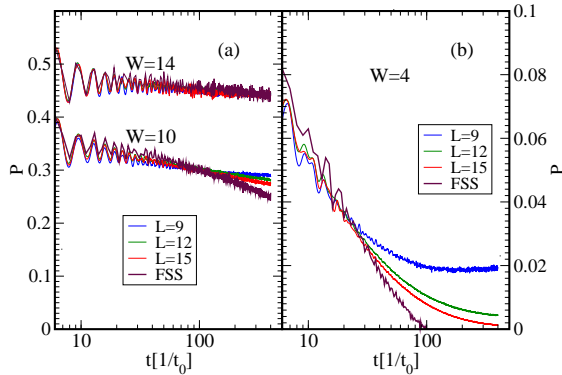


Figure S6. Charge imbalance P (as defined in Eq. (6) of the main text) vs. t of the t - J model with $L/3$ holes, equal number of spin-up and spin-down fermions at different values of random field, a) $W = 10$ and 14 and b) $W = 4$. Different sizes L are indicated in legends where in addition FSS indicates results where $1/L$ scaling was used separately for each point in time. Results in the case of $W = 14$ are essentially independent on the system size. Parameters of the system are $t = J = 1$. For time propagation a time step $\Delta t = 0.02$ was used. Note also different vertical scales in a) and b).

LIMITED FUNCTIONAL HILBERT SPACE FOR THE t - J MODEL

Approach, described in this section is only used for the case of time propagation of a system with a single hole. Results, obtained using this approximate method are presented in Fig. 1 and Fig. 2(a) of the main text. All other figures contain results obtained using complete Hilbert spaces. We first define generators of the Limited Functional Hilbert Space (LFS) that are simply off-diagonal parts of the Hamiltonian in Eq. (1) of the main text,

$$O_1 = \sum_{i,\sigma} c_{i+1,\sigma}^\dagger c_{i,\sigma} + H.c. \\ O_2 = \sum_i S_{i+1}^+ S_i^- + S_{i+1}^- S_i^+. \quad (\text{S8})$$

The generating algorithm starts from a hole at a given position, *e.g.* $i = 0$ in a Néel state of spins, $|\psi^{(0)}\rangle = c_{0\sigma}|\text{Neel}\rangle$. We then apply the generator of basis L -times to generate the LFS:

$$\{|\psi^{(l)}\rangle\} = (O_1 + \tilde{O}_2)^L |\psi_{(0)}\rangle, \quad (\text{S9})$$

for $l = 0, \dots, L$. The operator \tilde{O}_2 acts only on pairs of spins that due to hole motion deviate from the original Néel state. L essentially represents the largest distance that the hole travels from its original position. In the case of LFS we impose open boundary conditions. After completing generation of LFS we time evolve the wave function using the Hamiltonian in Eq. (1) of the main text while taking the advantage of the standard Lanczos-based diagonalization technique. Sizes of LFS span from $N_{\text{st}} \sim 10^4$ for $L = 21$ up to 6×10^4 for the largest $L = 29$ used in our calculations. To achieve sufficient accuracy of time propagation, we have used time-step-size ranging from $\Delta t = 0.1$ down to 0.02 and performed up to 4×10^4 time steps. In addition we have sampled over 10^3 different realizations of the random fields h_i .

The main advantage of LFS over the exact diagonalization approach is to significantly reduce the Hilbert space. The generation of spin excitations is obtained by the hole motion. The extent of spin excitations away from the hole position is of the order of $L/2$ and it exceeds the spin localization length ξ_s in the regime where $W \gtrsim 5$ by one order of magnitude see also Fig. S5. Results for different quantities computed using different L are presented in Figs. 1 (b) and (c) in the main text. The method has been successful in computing static and dynamic properties [43] as well as non-equilibrium dynamics [41, 42, 44] of correlated electron systems.

[1] R. Modak and S. Mukerjee, “Many-body localization in the presence of a single-particle mobility edge,” *Phys. Rev. Lett.* **115**, 230401 (2015).

- [2] C. Monthus and T. Garel, “Many-body localization transition in a lattice model of interacting fermions: Statistics of renormalized hoppings in configuration space,” *Phys. Rev. B* **81**, 134202 (2010).
- [3] D. J. Luitz, N. Laflorencie, and F. Alet, “Many-body localization edge in the random-field heisenberg chain,” *Phys. Rev. B* **91**, 081103 (2015).
- [4] F. Andraschko, T. Enss, and J. Sirker, “Purification and many-body localization in cold atomic gases,” *Phys. Rev. Lett.* **113**, 217201 (2014).
- [5] P. Ponte, Z. Papić, F. Huveneers, and D. A. Abanin, “Many-body localization in periodically driven systems,” *Phys. Rev. Lett.* **114**, 140401 (2015).
- [6] A. Lazarides, A. Das, and R. Moessner, “Fate of many-body localization under periodic driving,” *Phys. Rev. Lett.* **115**, 030402 (2015).
- [7] R. Vasseur, S. A. Parameswaran, and J. E. Moore, “Quantum revivals and many-body localization,” *Phys. Rev. B* **91**, 140202 (2015).
- [8] M. Serbyn, Z. Papić, and D. A. Abanin, “Quantum quenches in the many-body localized phase,” *Phys. Rev. B* **90**, 174302 (2014).
- [9] D. Pekker, G. Refael, E. Altman, E. Demler, and V. Oganesyan, “Hilbert-glass transition: New universality of temperature-tuned many-body dynamical quantum criticality,” *Phys. Rev. X* **4**, 011052 (2014).
- [10] E. J. Torres-Herrera and Lea F. Santos, “Dynamics at the many-body localization transition,” *Phys. Rev. B* **92**, 014208 (2015).
- [11] Marco Távora, E. J. Torres-Herrera, and Lea F. Santos, “Inevitable power-law behavior of isolated many-body quantum systems and how it anticipates thermalization,” *Phys. Rev. A* **94**, 041603 (2016).
- [12] C. R. Laumann, A. Pal, and A. Scardicchio, “Many-body mobility edge in a mean-field quantum spin glass,” *Phys. Rev. Lett.* **113**, 200405 (2014).
- [13] D. A. Huse, R. Nandkishore, and V. Oganesyan, “Phenomenology of fully many-body-localized systems,” *Phys. Rev. B* **90**, 174202 (2014).
- [14] M. Žnidarič, T. Prosen, and P. Prelovšek, “Many-body localization in the heisenberg XXX magnet in a random field,” *Phys. Rev. B* **77**, 064426 (2008).
- [15] J. H. Bardarson, F. Pollmann, and J. E. Moore, “Unbounded growth of entanglement in models of many-body localization,” *Phys. Rev. Lett.* **109**, 017202 (2012).
- [16] J. A. Kjäll, J. H. Bardarson, and F. Pollmann, “Many-body localization in a disordered quantum ising chain,” *Phys. Rev. Lett.* **113**, 107204 (2014).
- [17] M. Serbyn, Z. Papić, and D. A. Abanin, “Criterion for many-body localization-delocalization phase transition,” *Phys. Rev. X* **5**, 041047 (2015).
- [18] David J. Luitz, Nicolas Laflorencie, and Fabien Alet, “Extended slow dynamical regime close to the many-body localization transition,” *Phys. Rev. B* **93**, 060201 (2016).
- [19] M. Serbyn, Z. Papić, and D. A. Abanin, “Universal slow growth of entanglement in interacting strongly disordered systems,” *Phys. Rev. Lett.* **110**, 260601 (2013).
- [20] S. Bera, H. Schomerus, F. Heidrich-Meisner, and J. H. Bardarson, “Many-body localization characterized from a one-particle perspective,” *Phys. Rev. Lett.* **115**, 046603 (2015).
- [21] K. Agarwal, S. Gopalakrishnan, M. Knap, M. Müller, and E. Demler, “Anomalous diffusion and griffiths effects near the many-body localization transition,” *Phys. Rev. Lett.* **114**, 160401 (2015).
- [22] S. Gopalakrishnan, M. Müller, V. Khemani, M. Knap, E. Demler, and D. A. Huse, “Low-frequency conductivity in many-body localized systems,” *Phys. Rev. B* **92**, 104202 (2015).
- [23] Marko Žnidarič, Antonello Scardicchio, and Vipin Kerala Varma, “Diffusive and subdiffusive spin transport in the ergodic phase of a many-body localizable system,” *Phys. Rev. Lett.* **117**, 040601 (2016).
- [24] H. P. Lüschen, P. Bordia, S. Scherg, F. Alet, E. Altman, U. Schneider, and I. Bloch, “Evidence for Griffiths-Type Dynamics near the Many-Body Localization Transition in Quasi-Periodic Systems,” ArXiv e-prints (2016), [arXiv:1612.07173 \[cond-mat.quant-gas\]](https://arxiv.org/abs/1612.07173).
- [25] Jae-yoon Choi, Sebastian Hild, Johannes Zeiher, Peter Schauß, Antonio Rubio-Abadal, Tarik Yefsah, Vedika Khemani, David A. Huse, Immanuel Bloch, and Christian Gross, “Exploring the many-body localization transition in two dimensions,” *Science* **352**, 1547–1552 (2016), <http://science.sciencemag.org/content/352/6293/1547.full.pdf>.
- [26] P. Bordia, H. Lüschen, S. Scherg, S. Gopalakrishnan, M. Knap, U. Schneider, and I. Bloch, “Probing Slow Relaxation and Many-Body Localization in Two-Dimensional Quasi-Periodic Systems,” ArXiv e-prints (2017), [arXiv:1704.03063 \[cond-mat.quant-gas\]](https://arxiv.org/abs/1704.03063).
- [27] Wojciech De Roeck and François Huveneers, “Stability and instability towards delocalization in many-body localization systems,” *Phys. Rev. B* **95**, 155129 (2017).
- [28] P. Prelovšek, O. S. Barišić, and M. Žnidarič, “Absence of full many-body localization in the disordered hubbard chain,” *Phys. Rev. B* **94**, 241104 (2016).
- [29] R. Mondaini and M. Rigol, “Many-body localization and thermalization in disordered hubbard chains,” *Phys. Rev. A* **92**, 041601(R) (2015).
- [30] S. A. Parameswaran and S. Gopalakrishnan, “Spin-catalyzed hopping conductivity in disordered strongly interacting quantum wires,” *Phys. Rev. B* **95**, 024201 (2017).
- [31] S. Gopalakrishnan, K. Ranjibul Islam, and M. Knap, “Noise-induced subdiffusion in strongly localized quantum systems,” ArXiv e-prints (2016), [arXiv:1609.04818 \[cond-mat.dis-nn\]](https://arxiv.org/abs/1609.04818).
- [32] Janez Bonča and Marcin Mierzejewski, “Delocalized carriers in the tj model with strong charge disorder,” *Physical Review B* **95** (2017), [10.1103/physrevb.95.214201](https://arxiv.org/abs/10.1103/physrevb.95.214201).
- [33] Johannes Hauschild, Fabian Heidrich-Meisner, and Frank Pollmann, “Domain-wall melting as a probe of many-body localization,” *Physical Review B* **94** (2016), [10.1103/physrevb.94.161109](https://arxiv.org/abs/10.1103/physrevb.94.161109).
- [34] N.F. Mott, “Conduction in glasses containing transition metal ions,” *Journal of Non-Crystalline Solids* **1**, 1 – 17 (1968).
- [35] David Emin, “Phonon-assisted transition rates i. optical-phonon-assisted hopping in solids,” *Advances in Physics* **24**, 305–348 (1975), <http://dx.doi.org/10.1080/00018737500101411>.
- [36] Janez Bonča and Marcin Mierzejewski, “Delocalized carriers in the $t-j$ model with strong charge disorder,” *Phys. Rev. B* **95**, 214201 (2017).
- [37] J. Herbrych and J. Kokalj, “Effective realization of random magnetic fields in compounds with large single-ion anisotropy,” *Phys. Rev. B* **95**, 125129 (2017).
- [38] Anushya Chandran, Vedika Khemani, C. R. Laumann, and S. L. Sondhi, “Many-body localization and symmetry-protected topological order,” *Phys. Rev. B* **89**, 144201 (2014).
- [39] Andrew C. Potter and Romain Vasseur, “Symmetry constraints on many-body localization,” *Phys. Rev. B* **94**, 224206 (2016).
- [40] I. V. Protopopov, W. W. Ho, and D. A. Abanin, “The effect of $SU(2)$ symmetry on many-body localization and thermalization,” ArXiv e-prints (2016), [arXiv:1612.01208 \[cond-mat.dis-nn\]](https://arxiv.org/abs/1612.01208).

- nn].
- [41] M. Mierzejewski, L. Vidmar, J. Bonča, and P. Prelovšek, “Nonequilibrium quantum dynamics of a charge carrier doped into a mott insulator,” *Phys. Rev. Lett.* **106**, 196401 (2011).
 - [42] Denis Golež, Janez Bonča, Marcin Mierzejewski, and Lev Vidmar, “Mechanism of ultrafast relaxation of a photo-carrier in antiferromagnetic spin background,” *Phys. Rev. B* **89**, 165118 (2014).
 - [43] J. Bonča, S. Maekawa, and T. Tohyama, “Numerical approach to the low-doping regime of the t - J model,” *Phys. Rev. B* **76**, 035121 (2007).
 - [44] S. Dal Conte, L. Vidmar, D. Golez, M. Mierzejewski, G. Soavi, S. Peli, F. Banfi, G. Ferrini, R. Comin, B. M. Ludbrook, L. Chauviere, N. D. Zhigadlo, H. Eisaki, M. Greven, S. Lupi, A. Damascelli, D. Brida, M. Capone, J. Bonca, G. Cerullo, and C. Giannetti, “Snapshots of the retarded interaction of charge carriers with ultrafast fluctuations in cuprates,” *Nat. Phys.* **11**, 421–426 (2015).
 - [45] “See supplemental material at [url will be inserted by publisher] for the calculation of spin localization length, finite size analysis of results for finite hole doping, and the description of the limited functional space method,” .
 - [46] D. Schmidtke, R. Steinigeweg, J. Herbrych, and J. Gemmer, “Interaction-Induced Weakening of Localization in Few-Particle Disordered Heisenberg Chains,” ArXiv e-prints (2016), [arXiv:1607.05664 \[cond-mat.str-el\]](https://arxiv.org/abs/1607.05664).
 - [47] Y. Bar Lev, G. Cohen, and D. R. Reichman, “Absence of diffusion in an interacting system of spinless fermions on a one-dimensional disordered lattice,” *Phys. Rev. Lett.* **114**, 100601 (2015).
 - [48] T. Enss, F. Andraschko, and J. Sirker, “Many-body localization in infinite chains,” *Phys. Rev. B* **95**, 045121 (2017).
 - [49] J. T. Chayes, L. Chayes, Daniel S. Fisher, and T. Spencer, “Finite-size scaling and correlation lengths for disordered systems,” *Phys. Rev. Lett.* **57**, 2999–3002 (1986).
 - [50] Rahul Nandkishore and Andrew C. Potter, “Marginal anderson localization and many-body delocalization,” *Phys. Rev. B* **90**, 195115 (2014).
 - [51] R. Vosk, D. A. Huse, and E. Altman, “Theory of the many-body localization transition in one-dimensional systems,” *Phys. Rev. X* **5**, 031032 (2015).
 - [52] A. C. Potter, R. Vasseur, and S. A. Parameswaran, “Universal properties of many-body delocalization transitions,” *Phys. Rev. X* **5**, 031033 (2015).
 - [53] M. Mierzejewski, J. Herbrych, and P. Prelovšek, “Universal dynamics of density correlations at the transition to the many-body localized state,” *Phys. Rev. B* **94**, 224207 (2016).
 - [54] A. Pal and D. A. Huse, “Many-body localization phase transition,” *Phys. Rev. B* **82**, 174411 (2010).
 - [55] S. Bera, H. Schomerus, F. Heidrich-Meisner, and J. H. Bardarson, “Many-body localization characterized from a one-particle perspective,” *Phys. Rev. Lett.* **115**, 046603 (2015).
 - [56] M. Schreiber, S. S. Hodgman, P. Bordia, H. P. Lüschen, M. H. Fischer, R. Vosk, E. Altman, U. Schneider, and I. Bloch, “Observation of many-body localization of interacting fermions in a quasi-random optical lattice,” *Science* **349**, 842 (2015).